

Imaging glioma biology: Spatial comparison of APT, CBV, DTI and FET

Schön S¹, Cabello J², Yakushev I², Molina Romero M³, Metz M¹, Karimov I², Pyka T¹, Hock A⁴, Liesche F⁵, Gempt J⁶, Prebisch C¹, Zimmer C¹, Weber W² & Wiestler B¹

¹Department of Diagnostic and Interventional Neuroradiology, TUM University Hospital, Munich, Germany

²Department of Nuclear Medicine, TUM University Hospital, Munich, Germany

³Image-Based Biomedical Imaging, TUM, Munich, Germany

⁴Philips, Germany

⁵Department of Neuropathology, TUM University Hospital, Munich, Germany

⁶Department of Neurosurgery, TUM University Hospital, Munich, Germany

Introduction

Advances in glioma imaging have made it possible to not just capture anatomy, but the biology of tumors.

Besides well established techniques like DSC perfusion (measuring neoangiogenesis), diffusion-tensor imaging (reflecting cellular architecture) and FET-PET (visualizing protein synthesis), amide-proton transfer imaging (APT) has recently been introduced. APT measure the amide concentration and has been shown to correlate strongly with cellular proliferation.

Purpose

Given that these sequences measure partially overlapping biological processes, we aimed to investigate the spatial overlap of biological imaging modalities in a series of patients with newly-diagnosed gliomas.

Methods

We analyzed the preoperative MRI of 18 glioma patients with APT, 32-direction diffusion-tensor (DTI) and perfusion-weighted imaging (PWI). In addition, patients underwent static FET-PET imaging.

Post-processing encompassed calculating cerebral blood volume (nCBV) maps using AUC-based leakage correction (Hedderich et al., J. Neuroradiol, 2018), and signal deconvolution of DTI data. For the latter, we have previously developed a deep neural network (Molina Romero et al., MICCAI 2018) which estimates voxel-wise the tissue and free water fraction.

All images were rigidly co-registered using the ANTs toolkit. Images were manually segmented into contrast-enhancing tumor and FLAIR-hyperintense tumor. We took care to exclude necrotic areas from the segmentations.

We calculated patient- and voxel-wise Spearman correlation coefficients between all imaging modalities. In addition, we calculated Dice scores between tumor areas resulting from thresholding the imaging modalities using established cut-offs (FET > 1.6 TBR, nCBV > 2.5%, APT > 2, FA < 0.3 and Tissue volume > 0.5).

For each combination, we performed a one-sided t-test of the mean correlation among all 18 patients, and performed false-discovery rate adjustments using α .

Results

Of the 18 patients, 12 were diagnosed with an *IDH* wild type glioblastoma, 2 with an *IDH* mutant astrocytoma, 3 with an 1p/19q codeleted oligodendroglioma and 1 patient with a *BRAF* mutant pilocytic astrocytoma.

As we expected from the similar biological processes measured, APT and FET showed the highest correlation (Spearman's rho = 0.374, adj. p < 0.0001) in the FLAIR-hyperintense tumor. nCBV and the tissue volume fraction also showed a high correlation (Spearman's rho = 0.313, adj. p = 0.0002) in the FLAIR-hyperintense peritumoral area. FET and CBV were also positively correlated (Spearman's rho = 0.309, adj. p = 0.0006). Interestingly, APT and tissue volume fraction were negatively correlated in contrast-enhancing tumor (Spearman's rho = -0.238, adj. P = 0.009).

To investigate spatial overlap, we analyzed Dice scores between tumor areas defined through established cut-offs in the biological imaging modalities. In general, Dice scores were higher in contrast-enhancing than in FLAIR-hyperintense tumor. However, for predicting tumor growth and recurrence, the latter region is most interesting. Here, nCBV and tissue volume fraction had the highest overlap (Dice score = 0.53), followed by FET and CBV (Dice score = 0.428). APT had good overlap with CBV (Dice score = 0.406) and FET (Dice score = 0.398). We observed low spatial overlap for fractional anisotropy and tissue volume (Dice score = 0.295), APT and fractional anisotropy (Dice score = 0.286) and FET and fractional anisotropy (0.270).

Conclusion & Outlook

Voxel-wise, the PET signal was most strongly correlated with APT, followed by nCBV.

However, spatial analysis revealed that while there is relevant overlap between some sequences (like nCBV and tissue volume fraction or FET signal and nCBV), each modality also depicts unique areas within the tumor, as is expected from the different oncogenic processes they capture.

This highlights the potential of combining imaging information from different sequences to more accurately visualize tumor growth and infiltration.

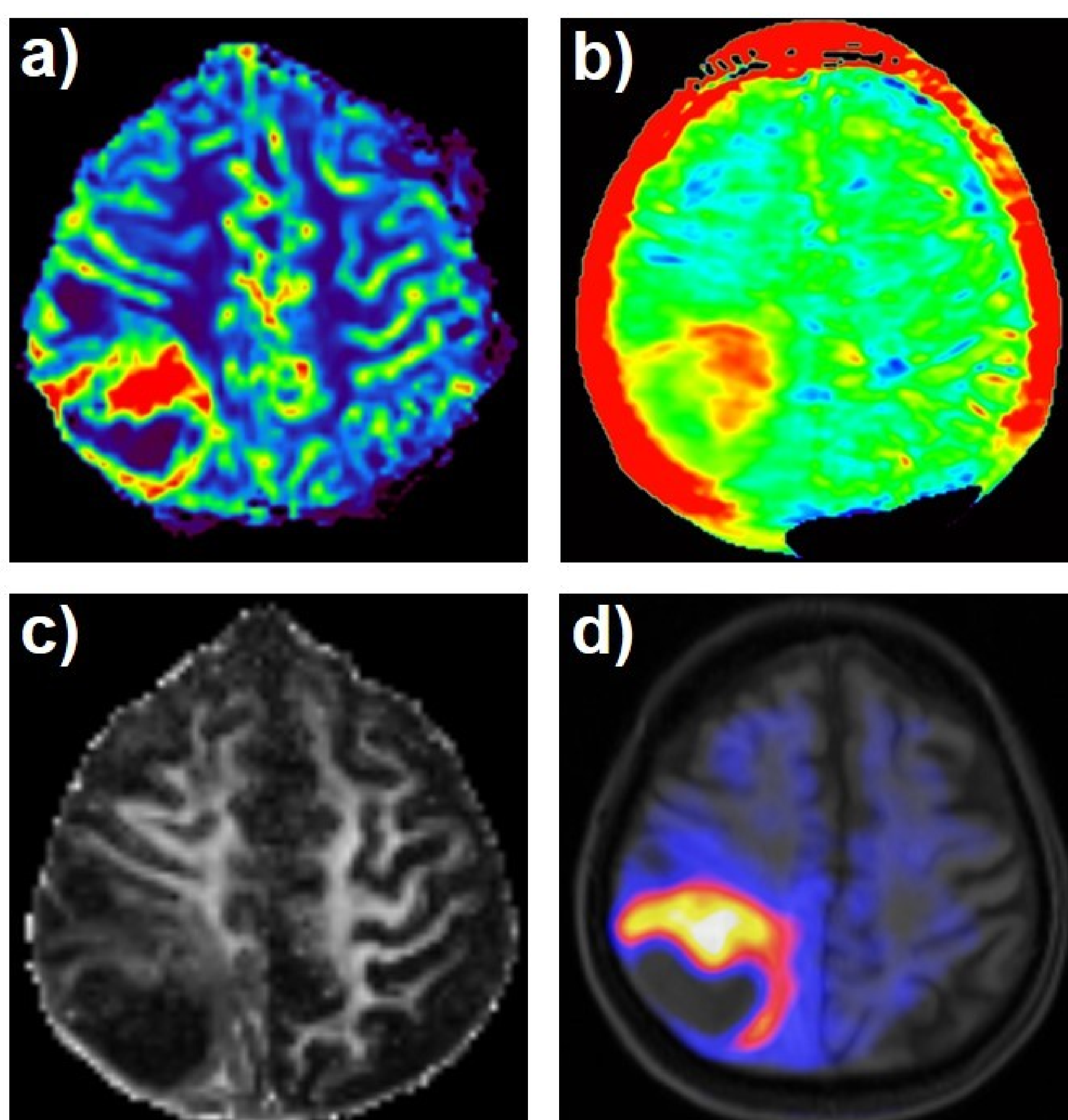


Figure 1: Examples of the imaging sequences analyzed: nCBV (a), APT (b), Fractional Anisotropy (FA) from DTI data (c) and FET-PET (d).

Reference:

Da Silva NA et al, Hybrid MR-PET of brain tumours using amino acid PET and chemical exchange saturation transfer MRI. Eur J Nucl Med Mol Imaging. 2018 Jun;45(6):1031-1040.